

PROCEEDINGS OF SPIE

SPIDigitalLibrary.org/conference-proceedings-of-spie

Optimization of multi-beam silicon photonics-based laser Doppler vibrometry for measuring cardiovascular signals on bare skin

Li, Yanlu, Aasmul, Soren, Morrissey, Padraic, Carey, Daniel, Wotherspoon, Tracy, et al.

Yanlu Li, Soren Aasmul, Padraic E. Morrissey, Daniel Carey, Tracy Wotherspoon, Petr Záruba, Roel Baets, "Optimization of multi-beam silicon photonics-based laser Doppler vibrometry for measuring cardiovascular signals on bare skin," Proc. SPIE 11621, Diagnostic and Therapeutic Applications of Light in Cardiology 2021, 116210A (5 March 2021); doi: 10.1117/12.2577159

SPIE.

Event: SPIE BiOS, 2021, Online Only

Optimization of multi-beam silicon photonics based laser Doppler vibrometry for measuring cardiovascular signals on bare skin

Yanlu Li^{*a,b}, Soren Aasmul^c, Padraic E. Morrissey^d, Daniel Carey^d, Tracy Wotherspoon^e, Petr Záruba^f, Roel Baets^{a,b}

^aPhotonics Research Group, Ghent University-imec, Technologiepark-Zwijnaarde 126, 9052, Ghent, Belgium; ^bCenter for Nano- and Biophotonics, Ghent University, Technologiepark-Zwijnaarde 126, 9052, Ghent, Belgium; ^cMedtronic Bakken Research Center, Endepolsdomein 5, 6229 GW, Maastricht, The Netherlands; ^dPhotonic Packaging Group, Tyndall National Institute, Lee Maltings Complex Dyke Parade, T12R5CP, Cork, Ireland; ^eMicrochip Technology Caldicot Limited, Phase 2, Castlegate Business Park, Monmouthshire, NP26 5YW, UK; ^fHolubova 978, 547 01 Nachod, Czech Republic

ABSTRACT

Non-invasive monitoring of cardiovascular diseases has been explored by means of laser Doppler vibrometry (LDV). In previous work, we have developed a handheld 6-beam on-chip LDV-device based on silicon photonics that can simultaneously measure the skin vibrations induced by cardiac action in multiple positions. This allows for the estimation of the pulse wave velocity (PWV), which is the current gold standard for evaluating arterial stiffness. The demonstrator has been used in a series of clinical feasibility studies. However, the system required the application of a retro-reflective (RR) patch to the skin prior to the measurement in order to enhance skin reflection. The use of the RR patch reduces the device usability and may also impact the measurement results.

In this work, we bring the concept one step further by eliminating the need for the RR patch during the measurement. The diffuse reflection from the skin leads to the low intensity of the back-reflected light detected by the interferometric readout system of the LDV. In order to increase the reflection signal level, we propose to operate the LDV at 1310nm where skin reflection is relatively strong while still being insensitive to skin tones. Furthermore, the optical imaging system between LDV-chip and skin has been designed for optimal signal strength in combination with sufficient depth of focus. We report on LDV measurements without using RR patch, and on the details of the optimized optical system.

Keywords: Cardiovascular disease monitoring, Laser Doppler vibrometry, Multi-beam Mach-Zehnder interferometer, photonic integrated circuit, silicon photonics

1. INTRODUCTION

Non-invasive monitoring of cardiovascular diseases (CVD) is of great interest in modern medical practice [1] and has been explored using laser Doppler vibrometry (LDV) in our previous Horizon 2020 project (CARDIS) funded by European Commission [2]. In the CARDIS project, we have developed a handheld LDV that can simultaneously measure the skin vibrations induced by the cardiac action at two locations (6 positions with a beam spacing of 5 mm at each location) [3-4]. Using the time delay of the same pulse arriving at different distances from the heart, we can estimate the value of the pulse wave velocity (PWV), which is the current gold standard for evaluating arterial stiffness [1]. The optical part of the LDV sensor is realized using a compact photonic-integrated circuit (PIC) based on a silicon-on-insulator (SOI) technology platform [5]. The primary advantage of realizing the optical components in SOI is that it is much easier to realize multi-beam LDV sensors compared to LDV sensors based on bulk optics or fiber optics. A multi-beam LDV can realize simultaneous multi-location measurement and hence reduce the alignment difficulty caused by the invisible locations of arteries under the skin. Because most optical components in this platform, such as optical splitters and grating couplers, have been developed mainly for operation at 1550 nm, the LDV demonstrated in the CARDIS project also uses this wavelength [4]. Since 1550 nm light is invisible, special red alignment beams were also implemented to indicate the locations of measurement spots. To ensure the distance between the sensor and the skin is

relatively constant, a spacer is also used. In order to enhance reflection, retro-reflective (RR) patches are applied to the skin at the measurement site before the measurement to enhance the reflection power. The RR patch is comprised of a layer of micro glass beads with a diameter of around 50 μm (3M-7610). The CARDIS LDV handpiece and a picture of a typical measurement position to capture local-carotid PWV in the neck are shown in figure 1. This demonstrator has been used in a series of clinical feasibility studies for local-carotid and carotid-femoral PWV measurements. The studies have shown that the handheld LDV can measure the carotid-femoral PWV with good accuracy compared to PWV values measured by standard PWV sensors [3].



Figure 1. (a) The CARDIS handheld LDV sensor with 2 x 6 beams at 1550 nm. The LDV sensor is developed in CARDIS project. (b) The measurement position of the LDV sensor for local-carotid PWV measurement. Reproduced from [3]

While it is highly beneficial for LDV operation at 1550nm, the RR patch was found to be a source of inconvenience as they had to be attached and removed for each measurement and their use limited the number of locations where PWV measurements could be performed. For these reasons, the clinical feasibility study in CARDIS recommended avoiding using the RR patches in future iterations of this device in order to ensure much faster and easier measurements. Furthermore, there are always some risks that the RR patches attached to the skin modify the displacement and vibration properties of the surrounding tissue. Based on this information, within our current project (European H2020 – InSiDe [6]), we are planning to fabricate a new LDV device that can measure pulse vibrations without using the RR patches. This new goal, however, also brings a lot of challenges to the LDV design because of the weak reflection from the skin. In the following part, we will outline our strategy to solve this problem.

2. PULSE VIBRATION MEASUREMENTS

In this section, we will discuss measurement signals obtained using the CARDIS LDV sensor, with and without RR patches. In the CARDIS LDV, each beam corresponds to one optical interferometer. Assume the amplitudes of the phasor describing the reference and measurement signals (before being sent to the target) are a and b respectively. The measurement signal will be sent to the target (the skin), reflected back to the PIC, and combined with the reference signal to generate a beating signal that can be detected by on-chip photo-diodes (PDs). Using a 90-degree optical hybrid [7] to combine the reference and measurement signals, two pairs of photocurrent signals are produced which can be represented by

$$I_{\pm}(t) = dc \pm \frac{1}{2} \eta \mu ab \cdot \cos(\theta(t) + \theta_{const})$$

$$Q_{\pm}(t) = dc \pm \frac{1}{2} \eta \mu ab \cdot \sin(\theta(t) + \theta_{const})$$

where η is responsivity of the PD, μ^2 is the reflection efficiency of the measurement signal in free space, $\theta(t) = 4\pi d(t)/\lambda$ is the phase change in the reflection signal due to Doppler effect, and $dc = \frac{1}{4} a^2 + \frac{1}{4} \mu^2 b^2$ represents the constant values. By subtracting the two signals with a 180-degree phase difference, we can get the I and Q signals which can be defined as:

$$I(t) = \eta \mu ab \cos(\theta(t) + \theta_{const}),$$

$$Q(t) = \eta \mu ab \sin(\theta(t) + \theta_{const}).$$

The displacement of the target can then be derived using the function $\arctan(Q/I)$ where the I and Q signals can form a Lissajous curve with a radius of $\eta\mu ab$. In addition, if the reference signal does not change and the root-mean-square noise of the I and Q signals (n_{rms}) are relatively constant, the noise of the LDV displacement is determined by the minimal detectable phase change in the IQ curve, $\delta\theta = \frac{n_{rms}}{\eta\mu ab}$, Where it can be seen that the noise floor of the LDV signals will decrease as the value of ηb increases. Therefore, one can improve the SNR of the LDV by enhancing the reflection efficiency of the measurement signal, or by increasing the optical power sent to the measurement beams.

The CARDIS LDV device has 12 sensing beams in total, and they are labeled as channels 11, 12, ... 16, 21, 22, ..., 26. The IQ curve of one typical pulse measurement on a candidate's neck (channel 23) with the RR patch in place is shown in figure 2(a). The data presented in this figure corresponds to a measurement time of 5 s with a sampling rate of 100 ksp/s. Notably, it can be seen that the IQ data does not form a distinct circular with a clear opening in the middle. This result is primarily attributed to the strong intensity variations in the reflection light. Therefore, while the RR patch can help to enhance reflection strength, it may still cause a problem when the reflections produce destructive interference at the receiver antenna. This result is typically known as a speckle problem [8]. Nonetheless, as mentioned above, the reflection can be estimated by the radius of each data point with respect to the center of the IQ curve. The histogram of the radii of all data points in the 5 s period is shown in figure 2(b), where the average value for the radius is around 7.1×10^{-2} V. It should be noted that the evolution of the radius as a function of time is presented in figure 2(c).

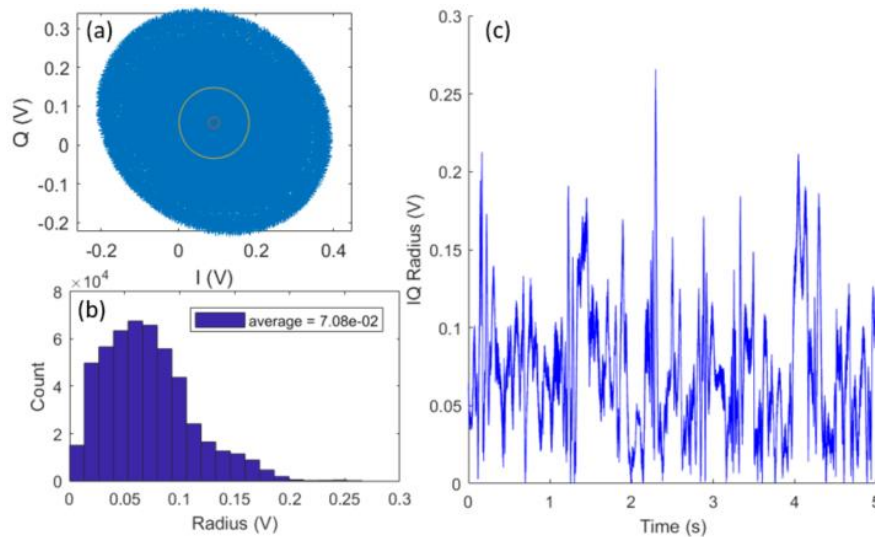


Figure 2. Measurement results from a candidate with help of RR patches. (a) The IQ Lissajous curve of channel 23 of the CARDIS LDV sensor, measuring pulses on the human neck with help of a retroreflective patch. (b) Histogram of the radii of the data points in the IQ curve. (c) The radius of the IQ data as a function of time.

The demodulated signals of two channels next to each other with a spacing of 5mm on the target skin are shown in figure 3(a). The corresponding velocity signals which correspond to the unfiltered derivative of the displacement signal are shown in figure 3(b). A lot of spikes can be seen in the unfiltered velocity values, and they are mainly caused by dynamic speckles [8]. Nonetheless, should be noted that speckle happens only for a very small portion of the signals, and they can be removed with low-pass filters or other speckle removing methods [8-9]. For example, the velocity signal with a 30 Hz low-pass filter is shown in figure 3(c), here, the velocity peaks of the pulses can be seen clearly. We also plot the histogram of the unfiltered velocity signal in figure 3(d). The red lines in figure 3(d) indicate the maximal velocity values observed in the filtered velocity signal ($= 5$ mm/s). It can be seen that the number of spikes with velocity values outside the velocity boundaries is really low.

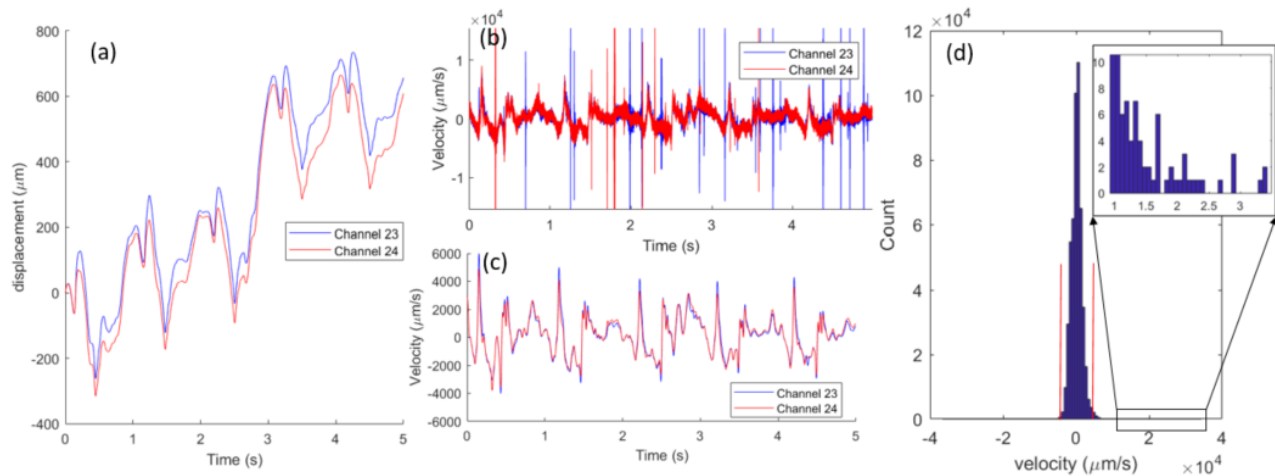


Figure 3. (a) Measured displacement signal of carotid pulses with help of RR patches at two adjacent locations with a spacing of 5 mm. (b) The velocity values of the pulses (without filter). (c) The velocity values of the pulses (with a 30 Hz lowpass filter). (d) Histogram of unfiltered velocity values.

If the RR patches are not used, it is usually not possible to get a meaningful LDV signal due to the low intensity of the back reflection from the skin which has a refractive index of around 1.37 at 1550 nm [10]. However, it is important to note that the skin boundary is not flat [11]. For instance, when the skin moves in the in-plane direction, the reflected light from the skin boundary will radiate to different directions in the time domain. Moreover, apart from the direct reflection at the skin boundary, most of the light signal goes inside of the skin and gets scattered and reflected. Meanwhile, the light can also be absorbed inside the skin, especially for 1550 nm which can be strongly absorbed by water [12]. The total reflection of 1550 nm in all directions is only around 5%. By comparison, RR patches can reflect up to 50% light. Furthermore, the RR patches can also ensure the reflection light is mostly sent back to the source location with a small spreading angle. Therefore, it is clear that the reflection from bare skin at 1550 nm will be reduced significantly compared to the case with a RR patch.

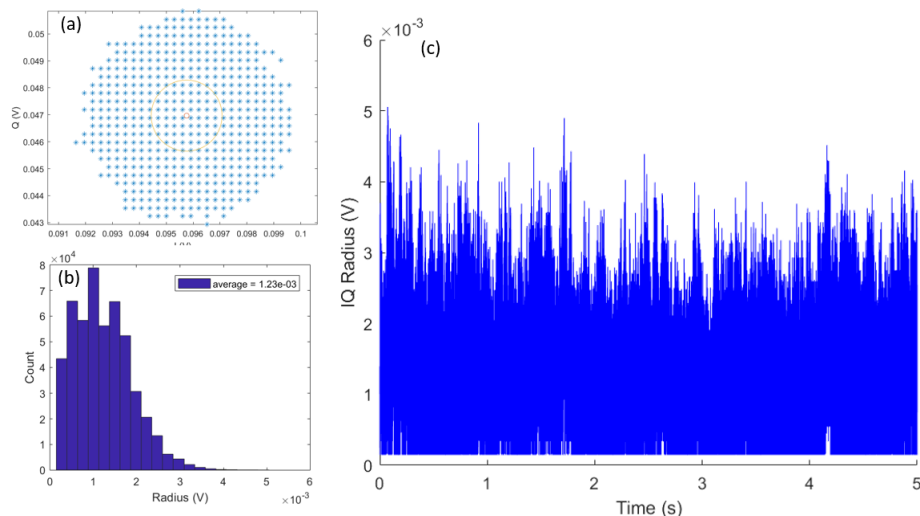


Figure 4. Measurement results from a candidate without RR patch. (a) The IQ Lissajous curve of the channel23 of the CARDIS LDV sensor, measuring pulses on the human neck with help of RR patch.

Despite these challenges, it is still possible to measure pulse vibrations for persons with a relatively strong skin reflection and we have recorded such measurements from a person without using an RR patch with the CARDIS LDV sensor. The IQ curve and the radius histogram from one such investigation are shown in figure 4(a) and figure 4(b). It was found that

the averaged radius of the measurement without RR patches are approximately 58 times less as compared to the one obtained with RR patches. That result suggests that the reflection power obtained directly from bare skin will be only around 1/3360 of that obtained with RR patches. However, it is still possible to get some useful signals in this case. The demodulated signals are shown in figure 5.

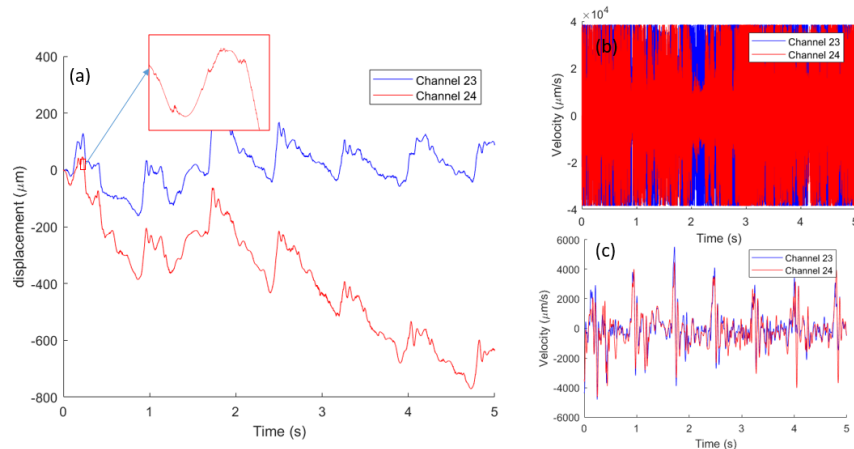


Figure 5. (a) Measured displacement signal of the carotid pulse at two adjacent locations with a spacing of 5 mm, without RR patches. (b) The velocity values of the pulses (without filter). (c) The velocity values of the pulses (with 30 Hz lowpass filter)

Although the demodulated signal presented in figure 5(a) has a lot of discontinuous points in the displacement values, the signal shape is qualitatively in agreement with the signals recorded using RR patches. In addition, we can see that the velocity signal (without filters) presented in figure 5(b) has too many spikes. There are two possible reasons for the presence of such spikes: dark speckle spots and low reflection strength. Since the optical system for the cases with and without RR patches is the same, the speckle size and movement will be very similar [13]. Therefore, the spikes shown in figure 5(b) are mainly caused by a reflection power that is too low. Alternatively, the signal presented in figure 5(c) shows the velocity signal filtered with a 30Hz low pass filter, and it shows clear and distinct peaks.

Furthermore, it is still possible to improve this signal by averaging the signals. It can be seen in figure 5(c) that the maximal speed is around 5 mm/s. According to Carson's bandwidth rule, the information of the useful signal is only in a bandwidth of 6.5 kHz. We can therefore reduce the noise by using a moving average process on the I and Q signals before demodulation. The updated demodulated velocity signals are shown in figure 6(a) for the case using a moving average over 7 samples. In particular, it can be seen that there are fewer spikes in the unfiltered velocity signal with respect to that demonstrated in figure 5(b). The corresponding filtered velocity signal is shown in figure 6(b). The histograms of velocity signals shown in figure 6(c) and 6(d) can indicate the performance of the moving average. Without a moving average, the portion of the velocity values that are within the boundary of 5mm/s is only 42%. So 58% of the captured signals are outside the boundaries of believable values and they are believed to be errors. After the moving-average, 94% of the data are within the believable boundary. That improvement is made because the total noise is reduced thanks to the moving average process. Notably, it seems that the noise level is very close to the signal level to have such an appreciable effect, so we can estimate that the noise level is around 1 mV or at least in the range of a few hundred micro-volts. In particular, if the reflection from the skin is even slightly reduced, we will not be able to obtain a demodulated signal. That's why the handheld LDV sensor cannot measure the pulsations of many candidates without the help of RR patches. Therefore, we can see that it is already possible to obtain reflections directly from bare skin, but only for some human skins with relatively strong reflection.

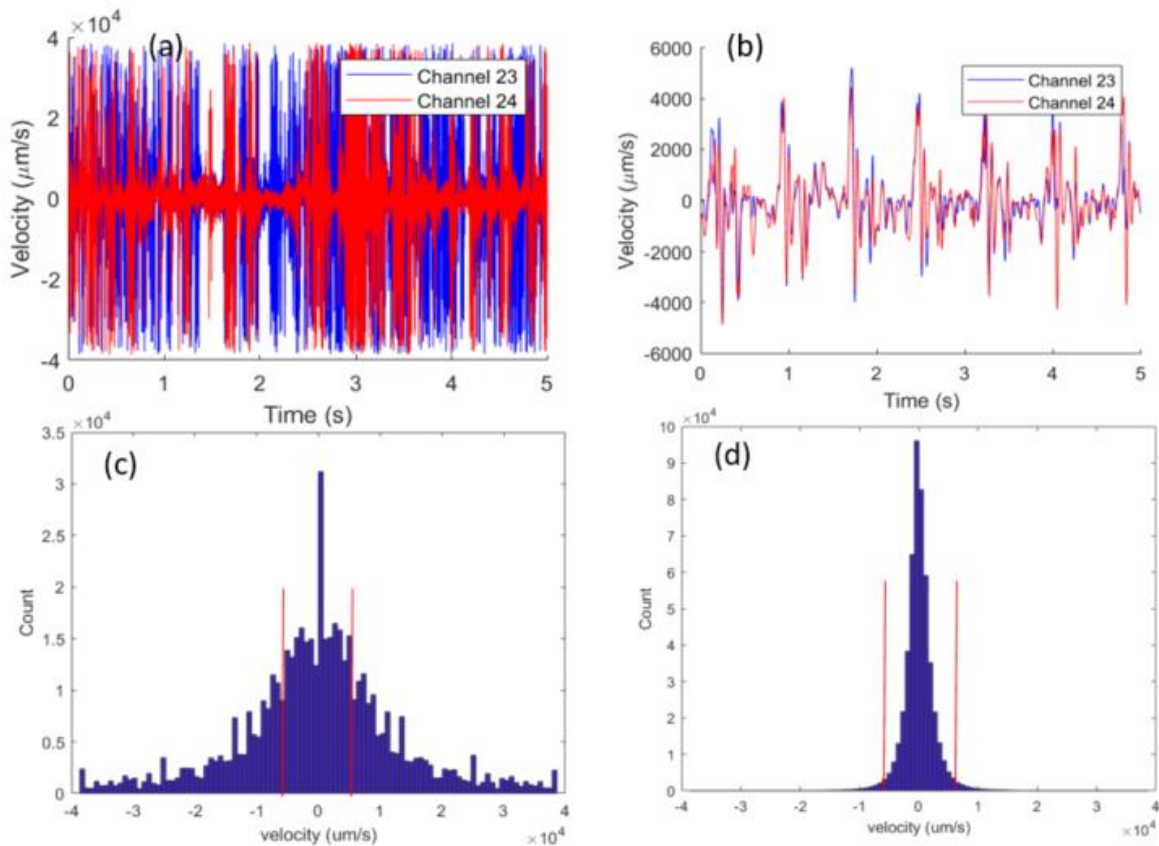


Figure 6. (a) Unfiltered velocity of the same data as is shown in figure 5.a. with a moving average filter on the I and Q data with a moving-average over 7 samples. (b) The corresponding velocity with a 30 Hz low-pass filter. (c) the histogram of unfiltered velocity values of data without using the moving-average filter. (d) the histogram of unfiltered velocity values of data with the moving-average filter.

3. IMPROVE REFLECTION POWER MEASUREMENT ON SKIN WITHOUT RETROREFLECTIVE PATCHES

To understand the reflection of human skin, the total reflectance of the skin has been measured by using a spectrophotometer. We have measured the optical reflection of the palm of four different subjects with different skin colors, the results are presented in figure 7. For one subject (T3) we measured the skin reflection from both the palm and the back of the hand. Note there are some sudden changes in the spectrum, which may be caused by the movement of the hand during the measurement. For another candidate (T4) we measured the palm with and without applied water to investigate absorption losses. Interestingly, it can be seen that the reflection in the visible range is generally strong, but depends strongly on the skin color. The observed reflection difference here is mainly caused by the difference in the amount of the natural pigmentation, melanin, present in the skin [12]. In contrast, the reflectance values for light with wavelengths longer than 1150 nm are not very different for different skin colors. The main reason for the less reflection is due to the absorption of water, which leads to local reflection minima at 1200 and 1400 nm. Because of the small measured deviation in skin reflection between subjects at 1550 nm, we do not expect large deviations in the reflection from the occurring skin types. Therefore, we can expect to obtain a proper signal level to obtain clear pulse vibrations for most people once we improve the reflection power of CARDIS device by more than 9 times.

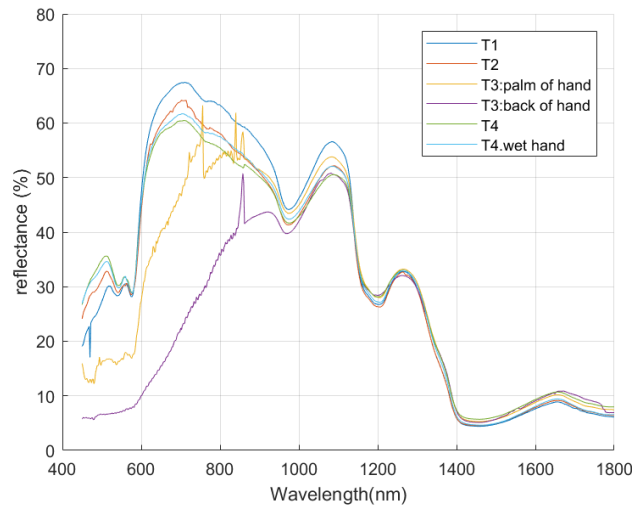


Figure 7. The reflectance of light from hand skins of four different candidates with different skin colors.

To further enhance the back reflection, we also propose to change the laser wavelength of the LDV from 1550 nm to 1310 nm. For example, it can be seen from figure 7 that the reflectance of skin at 1310 nm (30%) is around 6 times that of 1550 nm (5%). With the same amount of optical power illuminating the skin, a stronger reflection power would be expected, though most of the reflection enhancement is attributed to less absorption of water inside the skin. Another advantage of using 1310 nm is that the class 1 laser safety power is higher than that of 1550 nm. While the CW laser beam at 1550 nm has a 10 mW optical power limit for eye safety, that limit for 1310 nm is near 20mW [14]. In addition to this, a reduction from 6 to 4 beams will increase the optical power for each location by a factor of 1.5. The optical power of the input laser source will also be improved. We will use a laser source with 2.5 times more power (from 8 mW to 20 mW) in the first trial. Afterward, we will use a more powerful laser (up to 40 mW) to further increase the available SNR. As a result, the optical power of each measurement beam can be improved by a factor between 3.8 and 7.5. By combining the enhancement in both the optical power and reflectance, the total reflection power is expected to be enhanced by a factor of 22 at least.

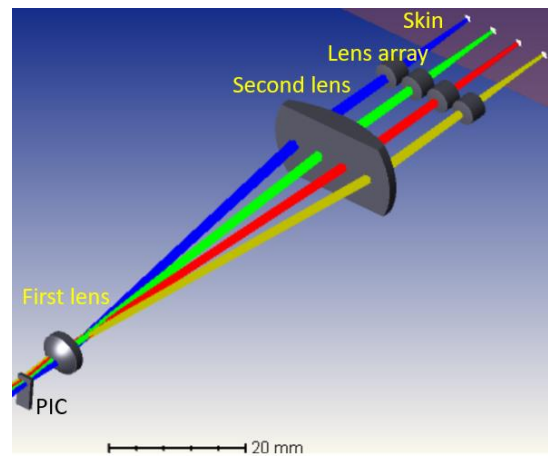


Figure 8. Lens system of InSiDe demonstrator. It comprises a first lens, a second lens, and a lens array.

To increase the detected amount of the diffusely scattered light backscattered from the skin, the magnification is reduced to increase the numerical aperture on the skin side. The optical system is shown in figure 8. The spot-spacing magnification of the system M_{spacing} is set to 10 resulting in an image of the four output beams (5mm separation) on the PIC onto skin positions with a 5mm spacing. The spot-size magnification of the sensor in the CARDIS device is $M_{\text{spot}}=16.7$, which is the same as the spot-spacing magnification of the CARDIS optical system, while the magnification

to be used in InSiDe device is just 2.8. This value is smaller than M_{spacing} , which is because the use of a lens array (see figure 8) ensures that the spot-spacing magnification and the spot-size magnification are decoupled. Since the effective cone of the reflection scales with $1/M_{\text{spot}}$, the total reflection power scales with $1/M_{\text{spot}}^2$. To enhance the reflection, one can use a lens system with smaller M_{spot} values. However, it must be noted that a smaller M_{spot} also corresponds to a larger focusing angle of the sensing beam on the target, which decreases the depth of focus (DOF). On one hand, the reflection power may be reduced as a result of the decrease of DOF, since the effective depths of skin that can reflect light to the PIC is reduced. On the other hand, the alignment procedure of the measurement becomes more challenging. Considering the aforementioned effects, we approximate that the total improvement in the optical could be increased between $M_{\text{spot}} (=6)$ and $M_{\text{spot}}^2 (=36)$ with the new magnification.

By combining all of the aforementioned improvements, the total reflection can be improved by more than 130 times. It is already possible to realize pulse measurement on various human skin types; However, if we use a higher optical power, it is possible to improve the reflection power by a factor upwards of approximately 1600, which will be nearly half of what is obtained in the case of the CARDIS system when used alongside the RR patches.

4. CONCLUSIONS

In this paper, we have outlined the method to improve the detection SNR of the proposed on-chip LDV that will be used to realize a noncontact pulsation detection without the help of using RR patches. The improvements include using a 1310 nm laser source with a stronger optical output power, using fewer measurement beams, and using an optical system with smaller spot-size magnification. For the InSiDe project, a reflection power improvement of 130 times or more is expected. An improvement of this magnitude will ensure the LDV measurement can be done directly on the bare skin without using RR patches.

5. ACKNOWLEDGEMENT

The authors acknowledge the H2020 InSiDe project (871547). The authors thank prof. Dirk Poelman for the photo-spectrometer measurements on human skins.

REFERENCES

- [1] The Reference Values for Arterial Stiffness' Collaboration, "Determinants of pulse wave velocity in healthy people and in the presence of cardiovascular risk factors: 'establishing normal and reference values'," *Eur. Heart J.* 31(19), 2338–2350 (2010).
- [2] <http://www.cardis-h2020.eu/>
- [3] Y. Li, L. Marais, H. Khettab, Z. Quan, S. Aasmul, R. Leinders, R. Schöler, P. E. Morrissey, S. Greenwald, P. Segers, M. Vanslembrouck, R. M. Bruno, P. Boutouyrie, P. O'Brien, M. de Melis, and R. Baets, "Silicon photonics-based laser Doppler vibrometer array for carotid-femoral pulse wave velocity (PWV) measurement," *Biomed. Opt. Express* 11, 3913-3926 (2020)
- [4] Y. Li, J. Zhu, M. Duperron, P. O'Brien, R. Schuler, S. Aasmul, M. De Melis, M. Kersemans, and R. Baets, "Six-beam homodyne laser Doppler vibrometry based on silicon photonics technology," *Opt. Express* 26(3), 3638–3645 (2018).
- [5] W. Bogaerts, R. Baets, P. Dumon, V. Wiaux, S. Beckx, D. Taillaert, B. Luyssaert, J. Van Campenhout, P. Bienstman, and D. Van Thourhout "Nanophotonic waveguide in silicon-on-insulator fabricated with CMOS technology," *J. Lightwave Technol.* 23, 401–402 (2005).
- [6] <http://www.inside-h2020.eu/>
- [7] R. Halir, G. Roelkens, A. Ortega-Monux, and J. Wanguemert-Perez, "High performance 90° hybrid based on a silicon-on-insulator multimode interference coupler," *Opt. Lett.* 36(2), 178 (2011).
- [8] S. Rothberg, B. Halkon, "Laser vibrometry meets laser speckle", *Proc. SPIE 5503*, Sixth International Conference on Vibration Measurements by Laser Techniques: Advances and Applications, (2004)

- [9] Y. Li, J. Zhu, M. Duperron, P. O'Brien, R. Schuler, S. Aasmul, M. De Melis, R. Baets, Speckle mitigation in laser Doppler vibrometry based on a compact silicon photonics chip, Conference on Lasers and Electro-Optics, United States, (2018)
- [10] T. Troy, S. Thennadil, "Optical properties of human skin in the near infrared wavelength range of 1000 to 2200 nm," J. Biomed. Opt. 6(2) (2001)
- [11] R. Ohtsuki, T. Sakamaki and S. Tominaga, "Analysis of skin surface roughness by visual assessment and surface measurement." OPT REV 20, 94–101 (2013).
- [12] M. Mendenhall, A. Nunez, and R. Martin, "Human skin detection in the visible and near infrared," Appl. Opt. 54, 10559-10570 (2015)
- [13] T. Asakura and N. Takai, "Dynamic Laser Speckles and Their Application to Velocity Measurements of the Diffuse Object" App. Phys. 25, 179-194 (1981).
- [14] IEC 60825-1:2014: Safety of laser products – Part 1: Equipment classification and requirements.